



INTERNATIONAL ATOMIC ENERGY AGENCY  
UNITED NATIONS EDUCATIONAL, SCIENTIFIC AND CULTURAL ORGANIZATION



INTERNATIONAL CENTRE FOR THEORETICAL PHYSICS  
34100 TRIESTE (ITALY) - P.O.B. 500 - MIRAMARE - STRADA COSTIERA 11 - TELEPHONE: 2360-1  
CABLE: CENTRATOM - TELEX 460892-1

H4.SMR/286 - 14

SECOND WORKSHOP ON  
OPTICAL FIBRE COMMUNICATION  
(14 - 25 March 1988)

ULTRASHORT PULSES IN FIBERS

A. Karasik  
Academy of Sciences of the USSR  
General Physics Institute  
Moscow, USSR

A.Ya.Karasik

The development of optical fibers having losses of just a few decibels per kilometer in early 70s initiated a qualitative jump in communication. The prospects of the data transmission with the rate of some Gbit/s for the distance of 10-20 km without a retranslator caused the real revolution in this branch of science and technique all over the world. However, as it turned out, the main problem at the creation of superbroadband transmission lines is not the fiber losses, but the effects of pulse broadening. It is known that the bit transmission is realized by the pulse signals. The bit rate of transmission is limited by the broadening of pulses which leads to their overlapping in time. In a linear system the bit rate of transmission, hence the channel capacity of an optical fiber is limited by the dispersive characteristic of the material and design of the optical fiber. "Nonlinear" lines, in which the parameters of pulses depend on the radiation power, are also considered in order to increase the bit rate of transmission.

In this lecture I shall describe some mechanisms of pulse broadening in linear and nonlinear regimes. First of all let us consider the important waveguiding parameters of fibers and unique properties of fused silica: which are the wide spectral range of transparency (0.4-1.8  $\mu\text{m}$ ), the presence of ranges of positive and negative group velocity dispersion in this region, the linear losses reaching 0.2 dB per km and some others.

#### Linear Propagation of Pulses in Fibers

The Gaussian pulse is usually chosen as a standard signal for the analysis of the pulse broadening:

$$I(t) = I_0 \exp[-(2t/\tau)^2] \quad (1)$$

Here  $I_0$  is the peak intensity in the maximum expressed in  $\text{W}/\text{cm}^2$ ,  $\tau$  is the total pulsewidth at the level of the  $I_0/e$ . The law of the Gaussian pulse broadening is written in the following way:

$$\tau_f = \sqrt{\tau_0^2 + \tau_g^2}, \quad (2)$$

here  $\tau_0$  and  $\tau_f$  are the pulsewidths at the fiber input ( $z=0$ ) and output ( $z=l$ ),  $\tau_g$  is the pulsewidth determined by the concrete broadening mechanisms. Or is the output pulsewidth when the input pulse has the form of  $\delta$ -function, i.e. at  $\tau_0 \ll \tau_g$ .

The top frequency of the pulse transmission determines the bit rate of transmission at binary coding:

$$G = \frac{1}{\tau_f \sqrt{|\ln \gamma|}}, \quad \text{bit/s} \quad (3)$$

$\gamma$  is the relative overlapping of neighbour pulses. For the certain separation of signals  $\gamma < 0.01$  is usually chosen ( $|\ln 0.01|^{-1/2} = 0.47$ ).

We must introduce the group delay of pulses when calculating the pulse broadening  $T = l/v_g$ , where  $v_g$  is the group velocity.

$$v_g = \frac{d\omega}{d\beta} = c \frac{dK}{d\beta} \quad (4)$$

Here  $\beta$  is the propagation constant of a mode,  $\omega$  is the light frequency,  $c$  and  $K=2\pi/\lambda$  are the light velocity and wave number in vacuum.

Now we have

$$T = l \frac{d\beta}{d\omega} = \frac{l}{c} \frac{d\beta}{dK} \quad (5)$$

It is convenient to introduce here the group refractive index

$$N_{ef} = \frac{d\beta}{dK}; \quad \frac{d(nK)}{dK} = n + K \frac{dn}{dK} \quad (6)$$

$$T = \frac{l}{c} N_{ef} \quad (7)$$

For the normal fiber prepared for the communication lines with the core-cladding refractive index difference of  $\Delta n = n_c - n$  we have

$$\frac{n_c - n}{n} = \frac{N_c - N}{N} \ll 1; \quad n \gg K \frac{dn}{dK}$$

The normalized effective refractive index of the linearly polarized LP mode is

$$b = \frac{\beta/K - n}{n_c - n} \quad (8)$$

Differentiating equation (6) and having in mind equation (8) we get equation (9)

$$N_{ef} = N + (N_c - N) \frac{d(V\beta)}{dV} \quad (9)$$

The normalized frequency is

$$V = \frac{2\pi}{\lambda} a \sqrt{n_c^2 - n^2} \quad (10)$$

where  $a$  is the radius of a core. The first part of equation (9) characterizes the material dispersion, the second part presents the group delay due to the mode dispersion. Physically the mode dispersion can be explained as follows. For the monochromatic excitation at the mode formation the whole number of wave vectors should be put between the two core-cladding boundaries. The change of  $\lambda$  results in a change of the wave vector value, that is why we should vary the slope of the beam so that a whole number of vectors will again be put between the two boundaries. The way of the beam and the mode delay are also changed in this case.

The derivative determining the difference of  $N_{ef}$  from  $N$  and  $N_c$  is shown in Figure 1. Near the cutoff the group velocity equals that in the cladding. At  $V$  increase the fields of modes are concentrated in the core and the wave runs slower than the plane wave in the material of a core. It is explained by the fact that it moves along the zigzag trajectory ( $N_{ef} > N$ ). At a significant increase of the normalized frequency the velocities of waves approach asymptotically the value of  $v_g = \frac{c}{N_c}$  ( $N_{ef} \rightarrow N_c$ ).

In a multimode fiber at uniform excitation of modes the deviation of delays  $\Delta T$  is determined by the difference of the maximal and minimal effective group indices  $\Delta T = \ell \Delta N_{ef} / c$ . We can assume that  $\Delta N_{ef} = N_c - N \approx n_c - n$  and the real deviation is  $\Delta T \approx 0.3 \ell \Delta n / c$ . For the typical multimode fiber  $\Delta n = 0.01$  and  $\Delta T = 3$  ns/km. In real fibers the modes of higher orders experience additional radiation loss. The deviation of time delays is also reduced because of the intermodal energy transfer.

The value of  $\Delta T = 3$  ns/km corresponds to the bit rate of only  $1.6 \times 10^8$  bit/s per 1 km. (H.-G. Unger. Planar optical waveguides and fibers. Clarendon Press. Oxford, 1977).

For example, in gradient fibers with the parabolic index profile the lengths of optical ways of different modes are equalized and the difference  $\Delta T$  is decreased. In gradient fibers the bit rate can reach 1 Gbit/s and more at the length of 1 km.

Let us now consider a single-mode fiber which excludes intermodal dispersion and allows to reach the record bit rates.

#### Single-Mode Fiber. Group Velocity Dispersion

For a single-mode fiber the group velocity dispersion (GVD) determines the rate of pulse spreading, and hence the bit rate. It can be obtained by differentiation of Eq. (6)

$$\frac{dN_{ef}}{dk} = \frac{d^2\beta}{dk^2} = c^2 \frac{d^2\beta}{d\omega^2} = c^2 \beta'' \quad (11)$$

The dispersion coefficient is defined as

$$K \frac{d^2\beta}{dk^2} = K \frac{dN}{dk} + \Delta N V \frac{d^2(V\beta)}{dV^2} \quad (12)$$

The first part of equation (12) determines the material dispersion, which is the same for all the modes. The second part presents the waveguide effects. In Eq. (12) a small term is omitted containing the derivative  $d\Delta N/dk$ . This derivative determines the dispersion of the profile - the dependence of the difference of group refractive indices on  $\omega$ .

The dispersion is small in silica glass having large window of transparency with the minimum of losses at  $\lambda \approx 1.5 \mu\text{m}$  (Figure 2). Figure 3 shows the dependence of the refractive ( $n$ ) and group ( $N$ ) indices on  $\lambda$ . Figure 4 illustrates the GVD dependence on  $\lambda$ . The zero value of GVD corresponds to the wavelength of  $\lambda_0 = 1.27 \mu\text{m}$  for pure  $\text{SiO}_2$ . At  $\lambda < \lambda_0$  we have a range of a normal or positive GVD, and at  $\lambda > \lambda_0$  - the range of anomalous or negative GVD. An addition of dopants into  $\text{SiO}_2$  results in a shift of  $\lambda_0$ . An addition of heavy in comparison with  $\text{SiO}_2$  molecules

(GeO<sub>2</sub>) shifts  $\lambda_0$  into the long wavelength range, and an addition of light molecules (B<sub>2</sub>O<sub>3</sub>) shifts it into the short wavelength range.

Figure 5 shows the dependence of the waveguide dispersion on the normalized frequency  $V$ . At  $V > 3$  this value is negative and partially compensates for the material dispersion. At  $V = 2.4$  the waveguide dispersion is of an order of  $10^{-3}$  and it can be neglected if compared with the value of  $dN/dk$  far from  $\lambda_0$ .

In the vicinity of the waveguide contribution into the dispersion value is higher and can shift the point of zero GVD. The dispersion of a profile also becomes very important in the vicinity of  $\lambda_0$  and can shift significantly the point of zero GVD up to 1.5  $\mu\text{m}$ .

The dispersion coefficient is expressed in ps/nm·km and the broadening parameter in a fiber can be written as

$$\Delta T = 120 \ell \Delta \lambda \quad (13)$$

where  $\Delta \lambda$  is the spectral width of radiation expressed in nm. The effect of GVD can be very large. For example, a spectral transform-limited pulse of 10 ps in width is broadened by more than 5 times at propagation in 10 km single-mode fiber ( $\mathcal{D} = 15\text{--}20$  ps/nm·km in a normal fiber at  $\lambda = 1.5 \mu\text{m}$ ).

At the propagation of a Gaussian pulse  $E_0(t) = \exp[-2(t^2/\tau_0^2)] \exp(i\omega_0 t)$  in a fiber along  $z$  axis the pulse shape remains Gaussian, and its duration  $\tilde{\tau}_z$  increases

$$\tilde{\tau}_z^2 = \tau_0^2 + 16(\beta'' z / \tau_0)^2 \quad (14)$$

and its amplitude decreases as the ratio  $\tau_0 / \tilde{\tau}_z$ .

At the dispersion length  $\ell_d$  the pulse is broadened by  $\sqrt{2}$  times

$$\ell_d = \frac{\tau_0^2}{4|\beta''|} \quad (15)$$

Thus, if a 10 ps pulse is doubled in width at the length of 1 km, then a 5 ps pulse doubles its width after 250 m of a fiber. Thus, the natural way to decrease the pulse broadening is to choose  $\lambda$  corresponding to the zero value of GVD ( $\lambda_0$ ). However, the pulse broadens even at  $\lambda = \lambda_0$ , which is associated with the influence of the higher order GVD  $\partial^3 k / \partial \omega^3$ . In this case the distance at which  $\tilde{\tau}$  is doubled is proportional to  $\tau_0^3$ . In reality it is very difficult to choose the source of radiation with  $\lambda = \lambda_0$ . Small deviations from  $\lambda_0$  (about 1%) deteriorate the bit rate by more than ten times.

For a definite length of the communication line we can achieve the minimal output pulsewidth  $\tilde{\tau}_\ell$  varying the input pulsewidth. In this case  $\tau_0^{\text{opt}} = 2\sqrt{\beta'' \ell}$ , and the pulse satisfying equation (15) appears to be the optimal one. For the line under consideration the output pulse

has the minimal width of  $\tilde{\tau}_\ell^{\text{min}} = 2\sqrt{2|\beta''|\ell}$  and the maximal bit rate of

$$G^{\text{max}} = 0.5 / \sqrt{2|\beta''|\ell} = 0.5 \sqrt{\pi c / \rho \lambda^2 |\partial^2 n / \partial \lambda^2|} \quad (16)$$

At  $\lambda = 1.5 \mu\text{m}$ ,  $\mathcal{D} = 20$  ps/nm·km,  $\gamma = 0.01$  and  $\ell = 100$  km we have  $G^{\text{max}} = 2.5$  Gbit/s.

#### Nonlinear Pulse Propagation in Fiber

In 1973 Hasegawa and Tuppert proposed to use nonlinearity of the refractive index of the fiber (Kerr effect) to compensate for the group velocity dispersion. The nonlinearity of the index can be written as:

$$n = n_0 + n_2 I \quad (17)$$

Here  $n_0$  - the refractive index in linear approximation,  $n_2 = 3.2 \times 10^{-16} \text{ cm}^2/\text{W}$  - a constant for fused silica. In spite of the small value of  $n_2$ , nonlinearity of  $n$  can be a powerful effect. The intensity  $I$  can reach the value of 1 megawatt per square centimeter at the radiation power of 1 W in a single-mode fiber with the core area of  $10^{-6} \text{ cm}^2$ . The nonlinear phase shifts can be very significant at big lengths of interaction of the radiation with silica. Different parts of pulse experience an additional phase shift at the propagation of a pulse with the phase  $\Phi(t) = \omega t - k z$  in a fiber of length  $\ell$  (effect of self-phase modulation (SPM)).

$$\Delta \Phi(t) = \frac{2\pi}{\lambda} \ell n_2 I(t) \quad (18)$$

The corresponding for  $\Delta \Phi(t)$  frequency shift  $\Delta \omega(t)$  is proportional to the derivative of the pulse envelope in time

$$\Delta \omega(t) = -\frac{d\Delta \Phi(t)}{dt} = -\frac{2\pi}{\lambda} \ell n_2 \frac{dI(t)}{dt} \quad (19)$$

As a result of SPM the pulse spectrum broadens, and the pulse acquires frequency modulation ("chirp"). It follows from (19) that the frequencies in the leading half of the pulse decrease (a Stokes shift) and in the trailing half - increase (an anti-Stokes shift). (Figure 6).

Let us assume that a pulse at the propagation along the fiber in the region of positive GVD acquires the chirp (Figure 6). When the beam with the chirp falls into the delay line on the base of two diffraction gratings (Figure 7), then "red" frequency components run after the diffraction longer distance than the "blue" frequency components. And as a result of the compensation of the time delay between these components, the pulse is compressed to the duration determined by the conversed width of the spectrum after SPM. For optimal compression

It is necessary to choose correctly the distance between the gratings. These methods of compression are actively investigated in many laboratories all over the world. Nowadays the shortest pulse of  $\tau = 6$  fs ( $6 \times 10^{-15}$  s) was achieved by this method. The compressed pulses can find application in a lot of different fields of science and technique.

Different materials can be used as media with the anomalous or negative dispersion, gases, liquids or a pair of diffraction gratings among them.

At the pulse propagation in a fiber, when dispersion is negative ( $K'' < 0$ ), the higher frequencies of the trailing half will overtake the lower frequencies of the leading half. This pulse will be collapsed in time. The evolution of the pulse envelope shape is governed by the nonlinear Schrödinger equation

$$i \frac{\partial E}{\partial z} + \frac{1}{2} \frac{\partial^2 K}{\partial \omega^2} \frac{\partial^2 E}{\partial t^2} - \frac{1}{2} \frac{\omega_0 n_2}{c} |E|^2 E = 0 \quad (20)$$

It has been analytically shown by Zakharov and Shabat (Sov. Phys. JETP; v. 37, 823, 1973) that equation (20) for  $K'' < 0$  has soliton solutions for the input pulses of a hyperbolic secant shape, and their amplitudes are integral multiples of the amplitude of the fundamental soliton

$$E(z=0, \tau) = \frac{1}{\Delta t_0} \sqrt{|K''| \frac{\lambda}{\pi n_2}} N \operatorname{sech} \left( \frac{\tau}{\Delta t_0} \right) \quad (21)$$

$\Delta t_0 = 0.568 \tau_0$ ,  $\tau_0$  - the pulse width,  $N$  - an integer. At  $N = 1$  we have the solution for a fundamental soliton. A fundamental soliton is a pulse which propagates in a lossless fiber without the evolution of the envelope shape. In this case the frequency shift due to the nonlinear change of the refractive index is exactly balanced with that which is due to the group dispersion.

At integers  $N = 2, 3, \dots$  ( $N = (P/P_0)^{1/2}$ ) a multisoliton pulse experiences periodic evolutions along the fiber length and periodically restores its shape (Figure 8). The soliton period is

$$Z_0 = \frac{\tau_0^2}{2|K''|} \quad (22)$$

The peak intensity corresponding to the fundamental soliton is

$$I = \frac{\lambda_0}{4n_2 Z_0} \quad (23)$$

These formulas are very important for practical estimations. In 1980 L.F. Mollenauer et al. (Phys. Rev. Lett., v. 45, p. 1095, 1980) for the first time experimentally investigated solitons in single-mode fibers. They used the pulses of 7 ps in width at  $\lambda = 1.55 \mu\text{m}$  of a sodium

chloride crystal colour center laser. According to (22) and (23) the power of the fundamental soliton  $P_0 \sim K''/\tau_0^2$ . In our case, if take into account the fiber parameters and  $\mathcal{D} = 15$  ps/nm·km,  $P_0 \approx 1$  W. For a 1 ps pulse the power  $P_0$  is essentially higher (about 50 W). It is clear that for communication the problem is the creation of semiconductor lasers with the pulsewidth of  $\tau = 1.7$  ps and the peak power of about 10 W. (We must take into account the fiber coupling efficiency as well). For a pulsewidth of  $\tau = 30$ -35 ps the power  $P_0$  will be 0.04 W at the same GVD. On the other hand, we can shift the zero GVD, for example, to  $\lambda = 1.5 \mu\text{m}$  by the variation of the refractive index profile. In this case at the reduction of  $K''$  (22) we can achieve the power of about 1 mW for 1-10 ps pulses as well. These values are quite real for the quickly developing semiconductor technology.

When nonlinearity dominates over the dispersion broadening of the pulse, multisoliton regime of pulse propagation can be used in communication lines. In this case the fiber length should equal the soliton period  $Z_0$  (22) (Figure 8). However, it is necessary to conduct experimental verification of the restoration of a multisoliton pulse shape at a few periods  $Z_0$ . It should be noted that for the input pulses of width  $\tau_0 = 30$  ps and close to zero GVD the period of a soliton can reach tens of kilometers. It is theoretically shown that the bit rate can be made an order of magnitude better than that of the best linear communication lines utilizing the wavelength at the zero group velocity dispersion.

Nonlinear regimes of the pulse propagation in a fiber give rise to a new important branch of science in the range of the ultrashort pulse formation. It is clear from Figure 8 that we can get the shortest pulse if we cut a fiber in the point of the quarter soliton period ( $z/Z_0 = 0.25$ ), that is in the point of the maximal compression. The degree of compression will increase with the increase of the soliton order  $N = \sqrt{P/P_0}$ . At large  $N$  theory gives the maximal degree of compression

$$\frac{\tau_0}{\tau} = 4.1 N \quad (24)$$

Soliton compression makes it possible to obtain 30-100-fold compression and to pass from pico- to femtosecond range of the time scale. Such investigations are conducted in USA (BTL), England and USSR (General Physics Institute, Academy of Sciences of the USSR).

High energy in the broad wings of the compressed pulse can be considered as one of the drawbacks of the soliton compression (see Figure 8). It is associated with the following fact. The "chirp" due to SPM is linear in the central part of the pulse and changes its sign at the pulse wings (Figure 6). It results in the compression of only the central part of the pulse. At  $N=20$  according to the calculations the degree of compression equals 82. But the compressed pulse will have only 17 percents of the energy, and 83 percents will contain the pedestal.

The method for the pulse compression without a pedestal was proposed and realized in the General Physics Institute of the Academy of Sciences of the USSR. This method introduces into the dynamics of the pulse propagation one more nonlinear process - that is stimulated Raman scattering.

The investigations of nonlinear regimes of pulse propagation in fibers allows to discover a great number of nice and novel effects. Unfortunately we can not consider all these effects in this short lecture.

The main problem for the soliton application in communication is, if it can exist in long fibers of tens of kilometers in length and with non-negligible losses? In the best fibers the losses are about 0.2 dB at the wavelength of 1.5  $\mu\text{m}$ . And the losses in 15 km-fiber are 3 dB/km, that is two times lower in intensity. The theory has examined the effect of a loss term. The loss term was added to the Schrödinger equation and treated as perturbation. It was shown that if the loss rate is not too great, then a soliton can be maintained. For example, for the losses of 3 dB the pulsewidth will increase by a factor of two. But if the losses are higher, a fundamental soliton can be destroyed.

There are some possibilities to amplify solitons in fibers with non-negligible losses. These possibilities are provided by the amplifiers on the base of semiconductor diodes and, for example, on the base of Raman amplifiers. Now I would like to remind you the principles of operation of a Raman amplifier. If we introduce, for example, in a silica fiber two laser frequencies  $\omega_1$  and  $\omega_2$ , and if  $\omega_1$  is more than  $\omega_2$ ; and if the difference  $\omega_1 - \omega_2$  equals the optical phonon frequency ( $\omega_1 - \omega_2 = \omega_{ph}$ ), then we shall have Raman amplification of a wave at the Stokes frequency  $\omega_2$ , which is described by the following equation

$$I_2 = I_s \exp(I_1 g - \alpha) l \quad (25)$$

Here  $g$  is the Raman gain,  $I_1$  is the pump intensity at the frequency

$\omega_1$ ,  $l$  is the length of a fiber,  $\alpha$  is attenuation in  $\text{cm}^{-1}$  and  $I_s$  is the intensity of the probe wave at the Stokes frequency  $\omega_2$ . Fused silica has a very nice, very broad spectrum of Raman amplification. This spectrum is determined by the overlapping of some inhomogeneously broadened phonon resonances and spreads practically from zero up to more than thousands of  $\text{cm}^{-1}$  (Figure 9). We can tune the difference of two frequencies in a wide range and can have effective amplification at a small pump power and large lengths of a fiber. At  $I_1 g l = 16$   $I_2$  equals  $I_2$ . The process of amplification will be effective when amplification exceeds losses  $I_1 g > \alpha$ . In BTL L.F. Mollenauer et al. demonstrated the compensation of loss by the Raman gain at a soliton propagation in a long fiber. The distortionless propagation of a 10 ps pulse (fundamental soliton) at  $\lambda = 1.56 \mu\text{m}$  along 10 km of a single-mode fiber was demonstrated (Opt. Lett., v.10, p.225, 1985).

In our laboratory in 1985 we proposed to use Raman amplification for the formation of Raman solitons at a Stokes frequency with a single-frequency pump wave. (JETP Lett., v.41, p.294, 1985; v.39, p.691, 1984). Now we shall consider the mechanism of this complicated process. At the propagation of a short pulse along a single-mode fiber in the region of negative GVD its spectrum is broadened due to SPM. We have a "chirp"-dependence of a frequency shift in time (Figure 10).

Some part of the broadened spectrum (the part of the low-frequency spectrum) falls in the range of Raman amplification of silica fibers, which spreads practically from zero. On the Stokes frequencies we have nonlinear slit which selects pulses shorter than the input pulse. Thus a pump pulse itself forms a sufficiently intense probe signal at the Stokes frequency. We called the proposed mechanism as a process of Raman amplification from the self-induced by means of SPM probe wave.

Recently this process was investigated theoretically in our laboratory and in BTL (USA).

In the range of the negative GVD the Stokes low-frequency pulse has the lower group velocity than that of the pump pulse. In the process of formation and propagation of the Stokes pulse it begins to delay relatively to the pump pulse, and effectively amplified in the field of nondepleted pump.

I have already told you that at the multisoliton propagation the compressed pulse has a high energy pedestal. In the regime under consideration the Stokes amplified pulse "eats up" the behind of the pump pulse pedestal. As a result, we can obtain a pedestalless powerful short compressed pulse at the Stokes frequency. This model was confir-

med by the experiments carried out in our laboratory.

In our experiments we used a parametric oscillator which generated 30 ps pulses tuned in the range of  $0.74 \pm 1.9 \mu\text{m}$ . As a result of the described nonlinear interaction in a long single-mode fiber, at the output of a fiber we selected femtosecond powerful pulses without a pedestal. From 30 ps pulses with the power of about 1 kW we obtained short pulses with the width of 100-200 fs and power of about 50 kW. We could tune these pulses by means of tuning of the pump pulses in the range from 1.5 to  $1.65 \mu\text{m}$ .

It is possible to form optical solitons in multimode fibers. These solitons have theoretically investigated in some works by Schvartsburg et al. (Sov. Quant. Electron., v.10, p.1059, 1983) and some of Italian scientists (Crosignani B., Di Porto P., Papas G.N., Opt. Lett., v.6, p.329, 1981; v.6, p.61, 1981).

But solitons in multimode fibers were not investigated experimentally. It is very interesting to discover experimentally these solitons.

And now I would like to discuss an important problem in the formation and measurement of ultrashort pulses with a "chirp". This problem deals with the radiation spectral filtering. The pulse frequency spectrum after SPM is given by the Fourier transform of pulse amplitude:

$$F(\omega) = \frac{1}{\sqrt{2\pi}} \int_{-\infty}^{\infty} P(t)^{1/2} e^{i\Delta\Phi(t)} e^{-i(\omega - \omega_0)t} dt \quad (26)$$

Here  $P(t)$  is the pulse power and  $\omega_0$  is the central frequency of radiation.  $\Delta\Phi(t)$  is the phase shift (18).

The frequency shift can be written as  $\Delta\omega(t) = \frac{d\Delta\Phi(t)}{dt} = -\kappa l n_2 \frac{dI(t)}{dt}$ . Figure 11 shows the spectrum of a Gaussian pulse at  $\Delta\Phi = 66$ . It is clear from this expression that the maximal frequency shift into the Stokes and anti-Stokes spectral regions can be achieved in the leading and trailing parts of the pulse in the inflection points of its envelope. In these points the "chirp" is absent ( $d\Delta\omega(t)/dt = 0$ ). If we realize spectral filtration of the extreme line in the spectrum, then an unmodulated pulse at the frequency shifted relatively to should correspond to this line. This assertion is confirmed by a simple modelling on a computer. It is clear from Figure 12 that at the spectral filtering of the extreme Stokes (or anti-Stokes) line in the leading (or trailing) fronts of the initial pulse a short spectrally-limited pulse is formed. The power of the selected pulse equals the power of the initial one. It should be noted that at the reduction of the slit width inside the extreme line the selected pulse remains spectrally-limited. At the increase of the slit width when some other lines are covered the selected pulse broadens and the time substructure emerges.

At the increase of the input pulse power with the growth of the phase shift, the duration of the selected pulse at optimal filtering decreases. For the values  $\Delta\Phi = 5, 60$  and  $250$  the ratios  $\tilde{\omega}_s/\tilde{\omega}$  equal 1.8; 4.7 and 7.5, respectively.

These calculations are confirmed by the results of our experiments. (JETP Lett., v.44, p.155, 1986). Figure 11 shows the spectrum of a 50 ps pulse at the output of a 0.5 m-long single-mode fiber. (We had the radiation of a garnet neodymium laser with  $\lambda = 1.06 \mu\text{m}$ ). At the input power in a fiber of about 20 kW, which corresponds to the phase shift of  $\Delta\Phi = 66$ , the theoretical spectrum agrees well with the experimental one.

At the output the collinear radiation broadened in a fiber at SPM is expanded into a spectrum by a diffraction grating. After the grating the beam acquires an elliptical form. For the restoration of the form the beam returns to the grating. Then by spatial filtering we can select the extreme (or some other) part of the beam. Using this method we have selected 10 ps pulses from the initial 50 ps ones.

By changing the phase shift value  $\Delta\Phi$  at the variation of the input power or the length of the fiber we can tune the wavelength of the selected pulses. The frequency shift is  $\Delta\omega = 0.5 \Delta\omega_0 \Delta\Phi$ .

At the generation of a second harmonic in a nonlinear crystal the width of the phase synchronism of the crystal is used as a spectral slit. The width of this slit may be varied over wide limits by the choice of different type crystals and by variation of the crystal length.

The method for the generation of a second harmonic in a nonlinear crystal is widely used for the measurement of the ultra-short pulse duration. Taking into account the data mentioned above, it is necessary to choose correctly the type and the thickness of the crystal, because it can distort the measured pulse duration.

The method of spectral filtering is very useful for the investigation of different aspects of the spectral-time conversions and for the control of the temporal characteristics of the pulse radiation. This method is discussed in the following papers: Nicolaus B. et al., Opt. Lett., v.8, No.3, p.189, 1983; Kitayama et al., Appl. Phys. Lett., v.45, No.6, p.838, 1984; Heritage J.P. et al., - " -, v.47, p.87, 1985; Weiner A.M. et al., Opt. Lett., v.11, No.3, p.153, 1986; Dianov E.M., Karasik A.Ya. et al., JETP Lett., v.40, p.148, 1984; JETP Lett., v.44, p.155, 1986, JETP, 1985.

#### Conclusion

We have discussed the physical aspects of some linear and nonlinear regimes of the ultrashort pulse propagation in silica fibers. We have considered the soliton regimes of propagation which can find

in the future application in superbroadband transmission lines. These regimes can be used for the pulsewidth tuning and for the formation of powerful femtosecond pulses, which is very important for the investigation of ultrafast phenomena in different branches of science and technique. Further prospects of these investigations are associated with the perfection of the picosecond diode lasers and photodetectors, with further investigations of a number of problems, as well as with the beginning of the experimental tests.

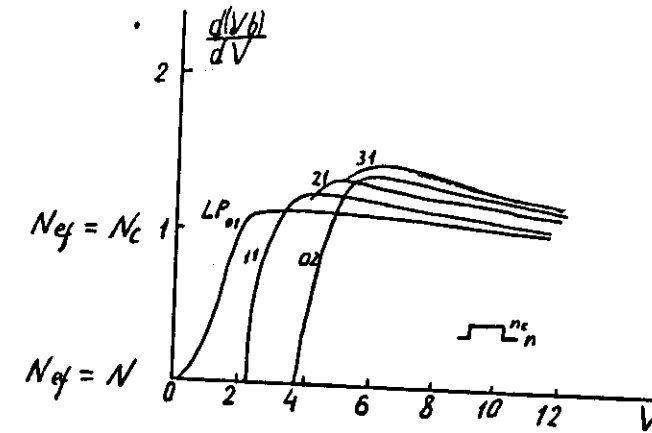


Fig.1 Normalized group delay as a function of  $V$

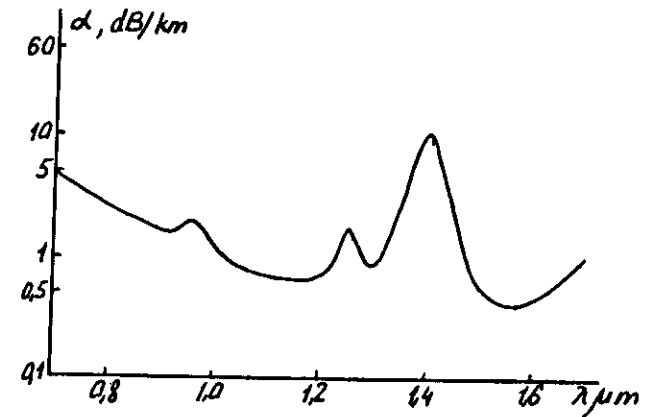


Fig.2 Typical singlemode fiber loss spectrum



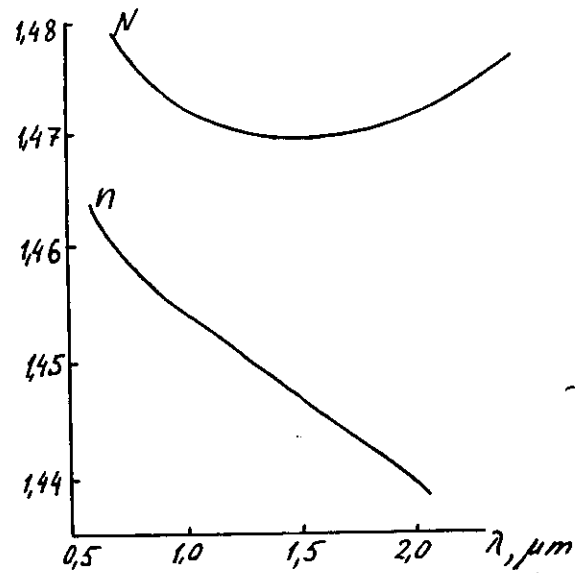


Fig.3 Refractive  $n$  and group  $N$  indices as function of wavelength for singlemode  $\text{SiO}_2$  fiber

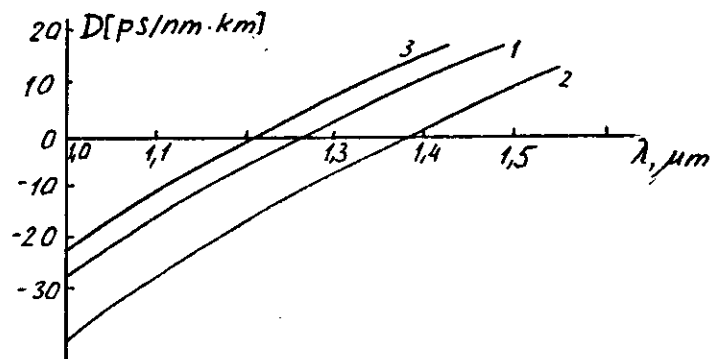


Fig.4 Wave length dispersion in singlemode fiber  
1-  $\text{SiO}_2$ , 2-  $\text{SiO}_2 + \text{GeO}_2$ , 3-  $\text{SiO}_2 + \text{B}_2\text{O}_3$

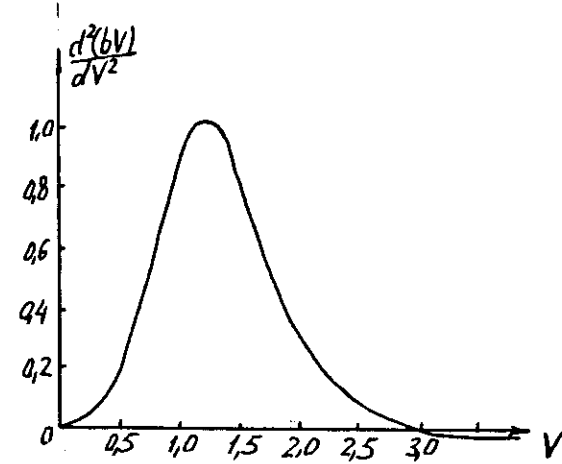


Fig.5 Waveguide dispersion on the normalized frequency

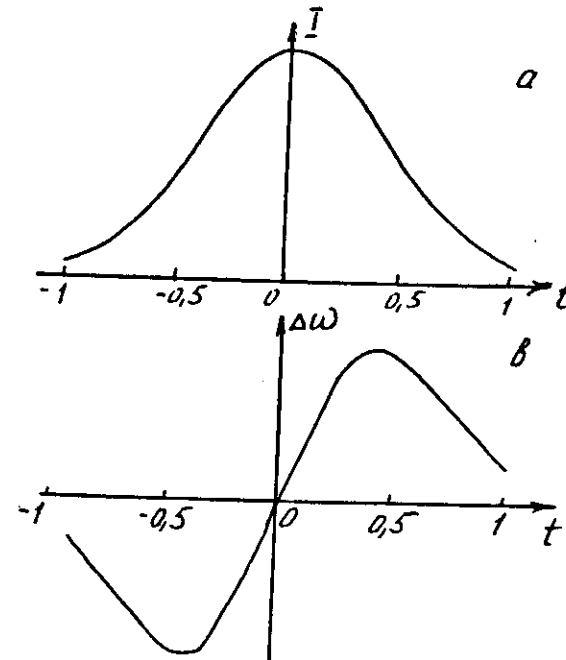


Fig.6 Optical pulse (a) and corresponding at SPM frequency chirp (b)

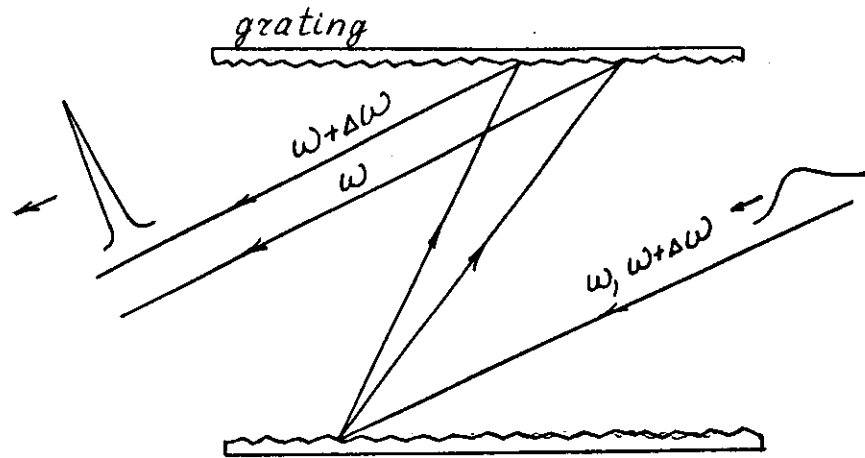


Fig.7 Grating compressor.

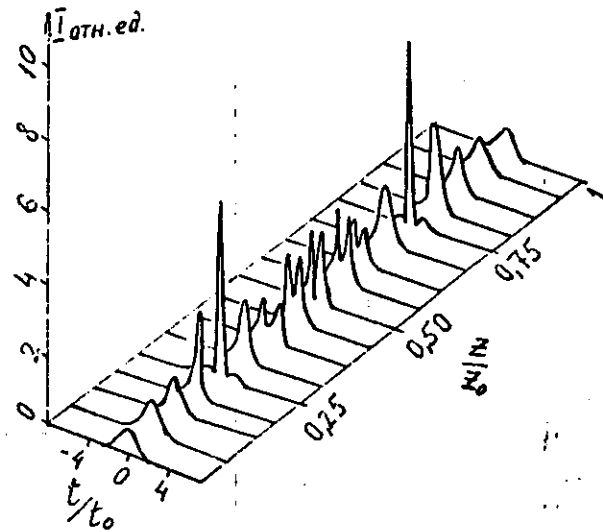
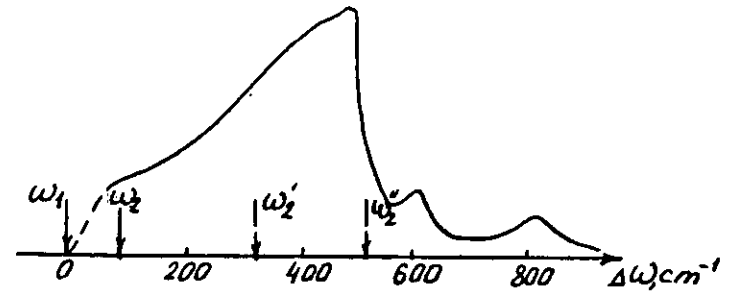
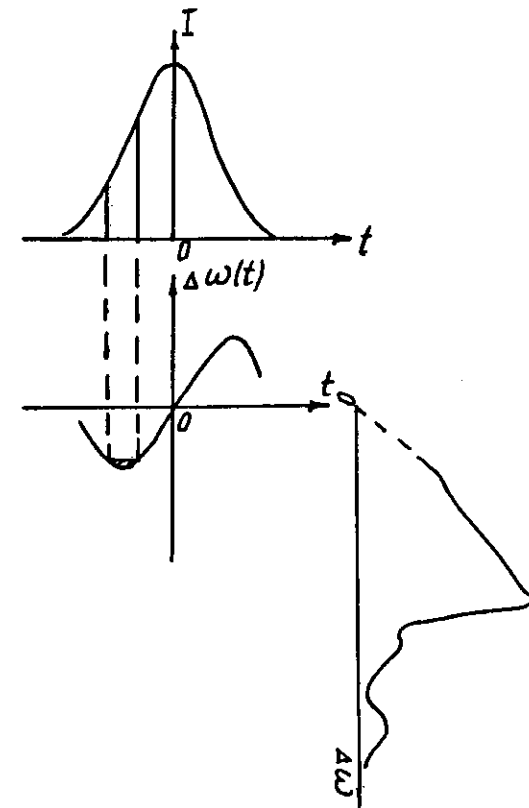
Fig.8 Theoretical behavior of higher-order solitons ( $N=3$ )Fig.9 Spectrum of Raman amplification  $\text{SiO}_2$   
 $\omega_1, \omega_2$  - pump and Stokes frequencies respectively

Fig.10 Formation of probe Stokes wave at Raman frequency

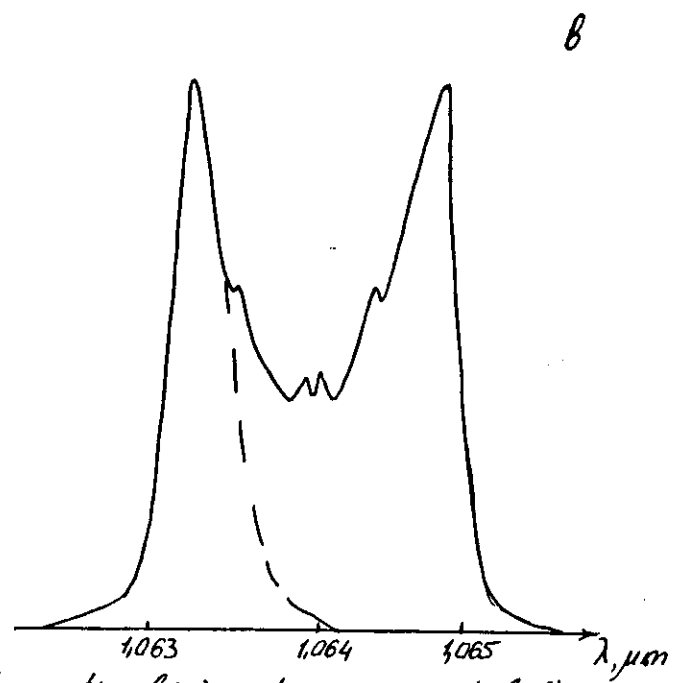
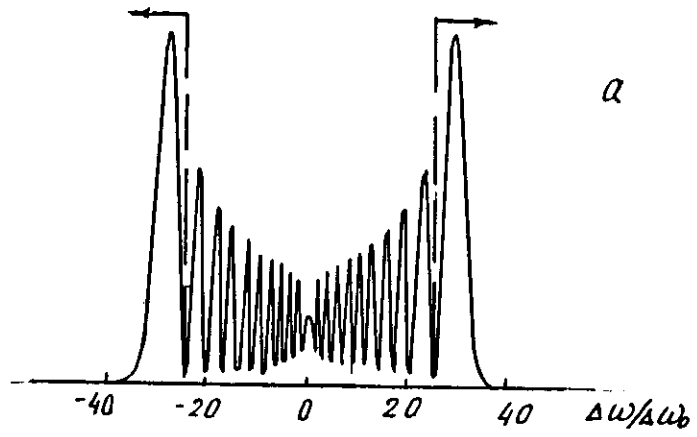


Fig. 11 Theoretical (a) and experimental (b) spectrum of radiation at SPM in short single-mode fiber

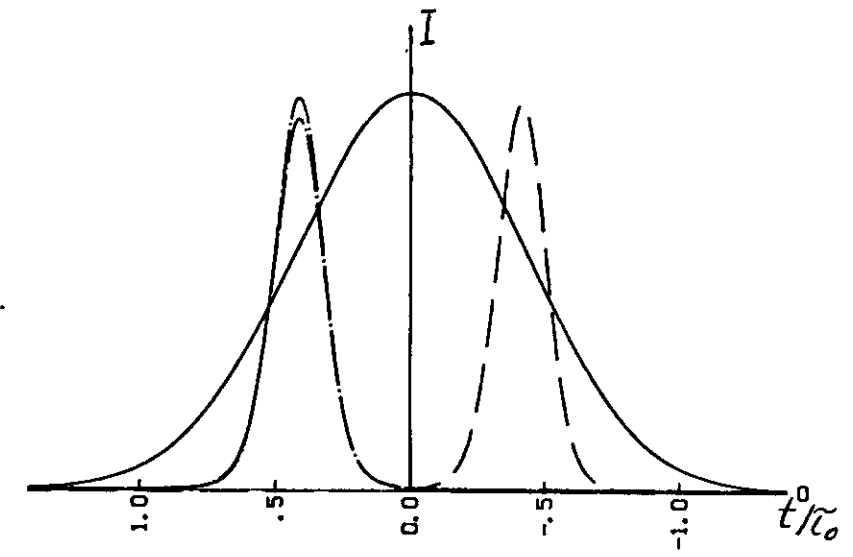


Fig. 12 Selection of Stokes(---) and anti-Stokes(-.-) pulses in a result of spectral filtration SPM radiation at output of single mode fiber

